Chemistry & Biology, Vol. 9, 195–202, February, 2002, ©2002 Elsevier Science Ltd. All rights reserved. PII S1074-5521(02)00104-7

A Mass Spectrometric Study of Metal Binding to Osteocalcin

Marjaana Nousiainen,[1] Peter J. Derrick,[2] Mari T. Kaartinen,[3] Pekka H. Mäenpää,[3] Juha Rouvinen,[1] and Pirjo Vainiotalo[1,4]
[1]Department of Chemistry
University of Joensuu
Post Office Box 111
FIN-80101 Joensuu
Finland
[2]Institute of Mass Spectrometry and
Department of Chemistry
University of Warwick
Coventry CV4 7AL
United Kingdom
[3]Department of Biochemistry
University of Kuopio
Post Office Box 1627
FIN-70211 Kuopio
Finland

Summary

Electrospray ionization Fourier transform ion cyclotron resonance mass spectrometry was used to investigate Ca^{2+}, Mg^{2+}, and La^{3+} binding to bovine bone osteocalcin (OCN). OCN was shown to bind 3 mol Ca^{2+} per mol protein. There was also evidence for the presence of four additional metal binding sites. Ca^{2+} increased the formation of the OCN dimer. Mg^{2+} bound to OCN to the same extent as Ca^{2+} but did not induce the dimerization of OCN. La^{3+} bound to a lesser extent than either Ca^{2+} or Mg^{2+} to OCN and, like Mg^{2+}, did not influence dimerization. Each Gla residue of OCN participates in Ca^{2+} binding, whereas Mg^{2+} binding may occur preferentially at sites other than Gla residues. This implies that the different natures of Ca^{2+}- and Mg^{2+}-containing OCN complexes influence the tendency of OCN to form a dimer.

Introduction

Osteocalcin (OCN) is a unique Ca^{2+} binding protein of 46–50 amino acid residues [1]. OCN is the most abundant noncollagenous protein in the mineralized extracellular matrices of bone and dentine. Synthesis of OCN in osteoblastic cells is regulated by the active metabolite of vitamin D, and the secreted protein is distributed to calcified tissues and, in nanomolar concentrations, to circulation [2]. The detailed functions of this small protein still remain unsolved. From the correlation between serum OCN level and bone formation, however, it has been proposed that OCN can be a specific measure of bone turnover [3, 4]. There is growing evidence that suggests that OCN plays an essential role in bone remodeling by reducing the process of excessive calcification [5–7].

[4]Correspondence: pirjo.vainiotalo@joensuu.fi

Common features of the OCN sequence are the Cys23-Cys29 disulphide bond and, in most species, the hydroxylated proline at position 9. The particular characteristic of the OCN sequence is the presence of three γ-carboxyglutamic acid (Gla) residues at positions 17, 21, and 24. These residues are produced by vitamin K-dependent protein carboxylation and are known to be required for Ca^{2+} and hydroxyapatite binding [8, 9]. By the way of exception, the sequences of human and wallaby OCN have been found to lack a γ-carboxylated glutamic acid residue at position 17 [10, 11]. OCNs in all species share an extensive sequence identity, and this establishes the structure and function relationship, which has been well-preserved during evolution. On the basis of predictive calculations based on the OCN sequence and circular dichroism (CD), UV and fluorescence titrations, and hydroxyapatite binding affinity studies, the OCN structure has been proposed to consist of two antiparallel α-helical domains connected by a β turn [12]. This structure is stabilized by one disulphide bridge. The Gla residues are orientated in the same direction in the N-terminal helix at intervals of 5.4 Å. This spacing is believed to promote Gla interactions with Ca^{2+} ions, which have the same spacing in the hydroxyapatite lattice of bone [1, 12–14].

Metal binding and conformational changes have been widely studied with OCN from different species by NMR, CD, UV and fluorescence spectroscopy, and equilibrium dialysis. OCN in solution has been demonstrated to bind from 1 to 6 mol of Ca^{2+} per mol protein, depending on the protein source and the ionic strength of the solution. An NMR study using dog bone OCN has established that the first two Ca^{2+} ions bind cooperatively with $K_{d\,Ca} \sim 10^{-4}$ M, and the additional Ca^{2+} binding with a slightly lower affinity stabilizes the osteocalcin structure [15]. Ca^{2+} binding induces a conformational change in OCN to create the full α-helical form [14, 16, 17] that greatly increases the affinity of the protein for hydroxyapatite [13]. The interaction of OCN with hydroxyapatite has been reported to be inhibited by the presence of Mg^{2+} [18]. OCN has also been shown to bind other alkaline earth metals as well as some transition metals and lanthanides with species-specific affinities and stoichiometries [12, 15, 19, 20].

In recent years, mass spectrometry (MS) has proved to be a very complementary technique to more traditional biophysical methods. Electrospray ionization (ESI) [21], which allows the transfer of thermally labile and nonvolatile analytes from aqueous solution to the gas phase and the production of gas phase ions under relatively gentle conditions, has allowed MS to be used in biopolymer studies [22, 23]. ESI-MS has been exploited in studies of noncovalent interactions of proteins because MS is a powerful analytical tool for detecting complex stoichiometries; this is because of its high accuracy in molecular-mass measurements [24]. ESI combined with Fourier transform ion cyclotron resonance (FTICR) mass spectrometry [25] provides higher mass resolution than other MS techniques, a fact that is essential for the

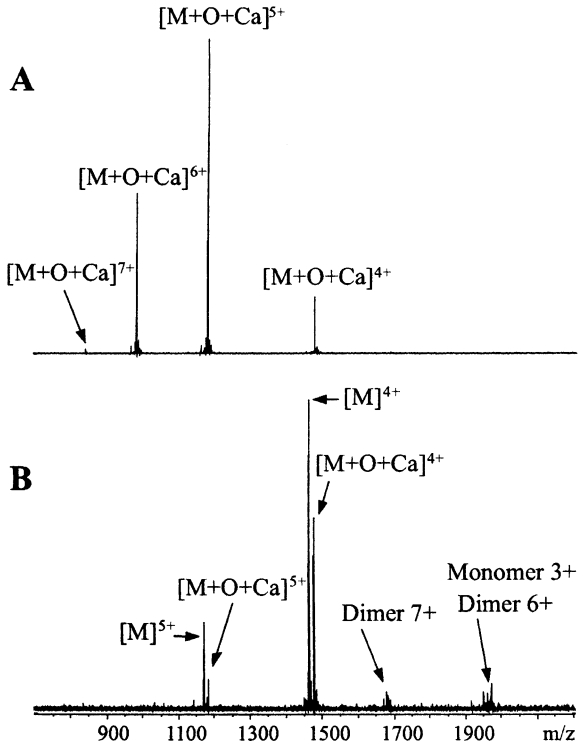

Figure 1. ESI-FTICR Mass Spectra of Apo OCN

OCN (15 μM) in (A) 1:1 water/acetonitrile containing 1% formic acid and (B) 5 mM ammonium acetate buffer (pH 5.8). M represents OCN.

identification of complexes containing multiple components [26–28]. A number of studies have also demonstrated that global conformational protein alterations resulting from changes in solvent conditions can be followed by means of electrospray charge state distributions [29]. The binding characteristics of various Ca^{2+} binding proteins, including calmodulin [30], calbindin [31], and parvalbumin [32] have been successfully analyzed with ESI-MS. The results have shown good correlations between mass-spectrometric measurements and data obtained by other bioanalytical methods.

In this study we have analyzed bovine bone OCN using ESI-FTICR mass spectrometry. The aim of the work was to obtain information on Ca^{2+} binding to OCN, on the complex stoichiometries, and on conformational changes due to metal binding. In addition, the binding of Mg^{2+} and La^{3+} to OCN was evaluated.

Results and Discussion

ESI-FTICR Mass Spectra of Apo Bovine OCN

We measured OCN both in highly acidic organic solvent and in aqueous buffer to obtain information on changes in electrospray charge state distribution. Figure 1 shows ESI-FTICR mass spectra obtained for bovine OCN in these different solution conditions. In water/acetonitrile (1/1, v/v) with 1% formic acid, OCN had a charge state distribution from the 7+ to the 4+ charge state, with the 5+ charge state being the most abundant (Figure 1A). We assume that OCN in the 7+ charge state is entirely protonated, i.e., one lysine, three arginines, two histidines, and the N-terminal tyrosine are protonated. In the ammonium acetate buffer (5 mM, pH 5.8), the charge state distribution shifted slightly to lower charges ranging from 5+ to 3+ (Figure 1B). The distribution was centered at around the 4+ charge state. In addition, an OCN dimer was detected at 7+ and 6+ charge states in ammonium acetate buffer. The charge state distribution obtained for OCN in organic solvent is proposed to correspond to a more open (i.e., unfolded) OCN conformation, compared to the conformation in the aqueous buffer.

The relative molecular mass measured for bovine OCN was 5849.71 ± 0.04. This figure was based on the most abundant OCN isotopes. This experimental figure agreed well with the average molecular mass (5850.37) calculated from the sequence. According to the measured molecular mass, OCN contained one disulphide bond, one hydroxylation, and three carboxylations in both solvents.

There was evidence of a species having a mass of 53.91 u higher than the mass of OCN. This species gave the major peaks in the mass spectrum when organic solvent was used (Figure 1A). As reported below, this species both decarboxylated under collision-induced dissociation (CID) and bound Ca^{2+} in the same manner as OCN. The addition of EDTA to OCN solution removed the mass shift of 53.91 u and introduced new weaker peaks representing a species that was 16.0 u higher in mass than OCN. These new peaks, giving a derived mass of 5865.71 u, are proposed to be due to an oxygen atom in the sequence. Because the signal corresponding to OCN+O was weak, it is supposed that treatment with EDTA removed the oxygen beside Ca^{2+}. We digested OCN by endoproteinase Asp-N in order to determine the position of an oxygen in the sequence. However, no oxygen was present in the produced peptides. Thus, the position of the oxygen remained uncertain. Our conclusion is that the mass shift of 53.91 u is produced by an adduct of one residual Ca^{2+} ion (and the corresponding loss of two protons) and by one oxidation of the protein. The theoretical mass of O+(Ca-2H) (53.94 u) is in agreement with the mass spectrometrically determined mass difference of 53.91 u.

Figure 2 illustrates the fragments, resulting from ion-source CID, of OCN–O–Ca in the 4+ charge state. The sample was dissolved in organic solvent, and the potential applied to the capillary was increased incrementally in 24 V steps from 56 V to 128 V. The collision-induced dissociation in the ion-source resulted in stepwise loss of up to three times 43.99 mass units. This mass loss is ascribed to CO_2 originating from the three Gla residues. The loss of the first CO_2, i.e., the putative decarboxylation of the dicarboxylic side chain of a Gla residue, took place to a significant extent upon the increase of capillary potential from 56 V to 80 V (see Figures 2A and 2B). The species containing two intact Gla residues appeared to be more stable than the species containing either one or no intact Gla residue. The proposed decarboxylations of the other two Gla residues took place together at 128 V (Figure 2D). This observed facile fragmentation of Gla is consistent with previous reports showing that under both low- and high-energy CID

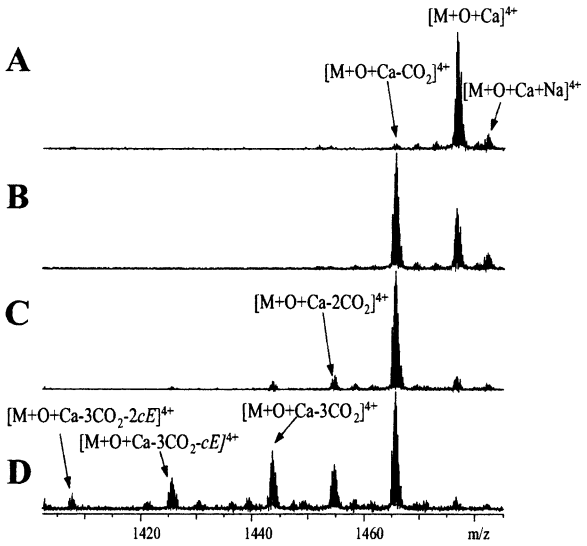

Figure 2. Collision-Induced Dissociation of Apo OCN

Expanded ESI-FTICR mass spectra of the 4+ charge state of OCN (15 μM) in 1:1 water/acetonitrile containing 1% formic acid as a function of capillary potential. M represents OCN and *cE* represents the side the chain of glutamic acid.

(A) 56 V.

(B) 80 V.

(C) 104 V.

(D) 128 V.

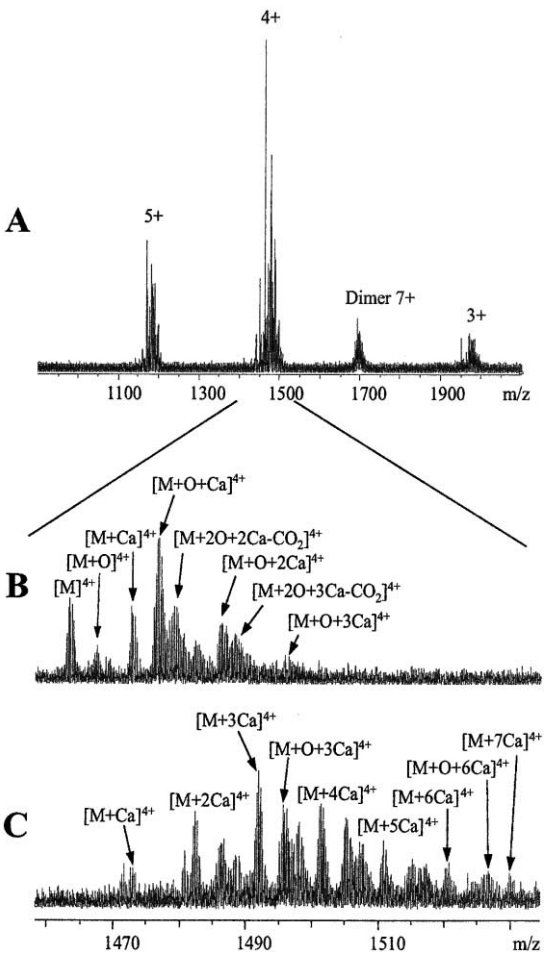

Figure 3. ESI-FTICR Mass Spectra of OCN in the Presence of Calcium

$CaCl_2$ concentration being (A and B) 0.1 mM and (C) 1.0 mM. Panels (B) and (C) show the expansion of the 4+ charge state. The data were recorded on a 15 μM protein sample in 5 mM ammonium acetate buffer (pH 5.8). M represents OCN.

γ-CO_2 is lost before any peptide backbone bond fragmentation [33, 34]. In addition, at a capillary potential of 128 V, losses of 72.0 and 144.0 mass units were observed. This can be explained as a loss of one and two propenoic acids from the side chains of decarboxylated glutamic acid residues. The oxygen atom and Ca^{2+} remained in the protein and were not lost as a result of ion source CID. This would suggest that the residual Ca^{2+} is not bound to any of the three γ-carboxylic acid moieties of Gla residues.

Ca^{2+} Binding to Bovine OCN

We measured spectra of OCN and $CaCl_2$ at different concentration ratios ranging from 1:0.7 to 1:67. Figure 3A shows the whole of the ESI-FTICR mass spectrum obtained for an OCN solution containing 0.1 mM $CaCl_2$ (OCN to $CaCl_2$ ratio was 1:6.7) in ammonium acetate buffer. The presence of Ca^{2+} did not significantly change the charge state distribution of the OCN monomer. Ca^{2+} binding was similar for the 5+, 4+, and 3+ charge states. The same numbers of Ca^{2+} ions were bound to the protein in each charge state. The mass difference between two consecutive Ca^{2+}-containing species was 37.951 u, which indicates that the binding of each Ca^{2+} ion to OCN was accompanied by the loss of two protons. This measured mass difference agrees well with the calculated mass (37.948 u) for Ca^{2+} with two protons displaced. Given neutralization of the Ca^{2+} charge, the charge balance of the protein would be maintained. To simplify the assignment of the detected species, we did not write added or lost protons in labels of the species. Thus, for example, $[M+O+3Ca]^{4+}$ represents $[(OCN+O+3Ca\text{-}6H)+4H]^{4+}$; in other words, M stands for the OCN protein, O for oxygen, and Ca for calcium, respectively.

Ca^{2+} binding is illustrated in greater detail in Figures 3B and 3C, which show the expanded 4+ charge state of the ESI-FTICR mass spectra obtained for OCN samples containing 0.1 and 1.0 mM $CaCl_2$ (protein to metal concentration ratios of 1:6.7 and 1:67). In the presence of 0.1 mM $CaCl_2$, the most intense peak remained that due to $[M+O+Ca]^{4+}$, which corresponds to OCN–O–Ca complex in the 4+ charge state (Figure 3B). OCN bound either one or two Ca^{2+} ions, and OCN–O bound one, two, or three Ca^{2+} ions. In addition, we observed a peak assigned to OCN with a loss of CO_2, which presumably cleaved from a Gla residue, and an incorporation of two oxygen atoms and two or three Ca^{2+} ions. It should be noted that an increase in the $CaCl_2$ concentration from 0.1 mM to 1.0 mM (Figure 3C) led to a greater relative intensity of the peaks assigned to OCN associated with Ca^{2+} ions without incorporation of an oxygen atom. At a 1.0 mM concentration of $CaCl_2$, there was no signal in the spectrum corresponding to OCN free of Ca^{2+}.

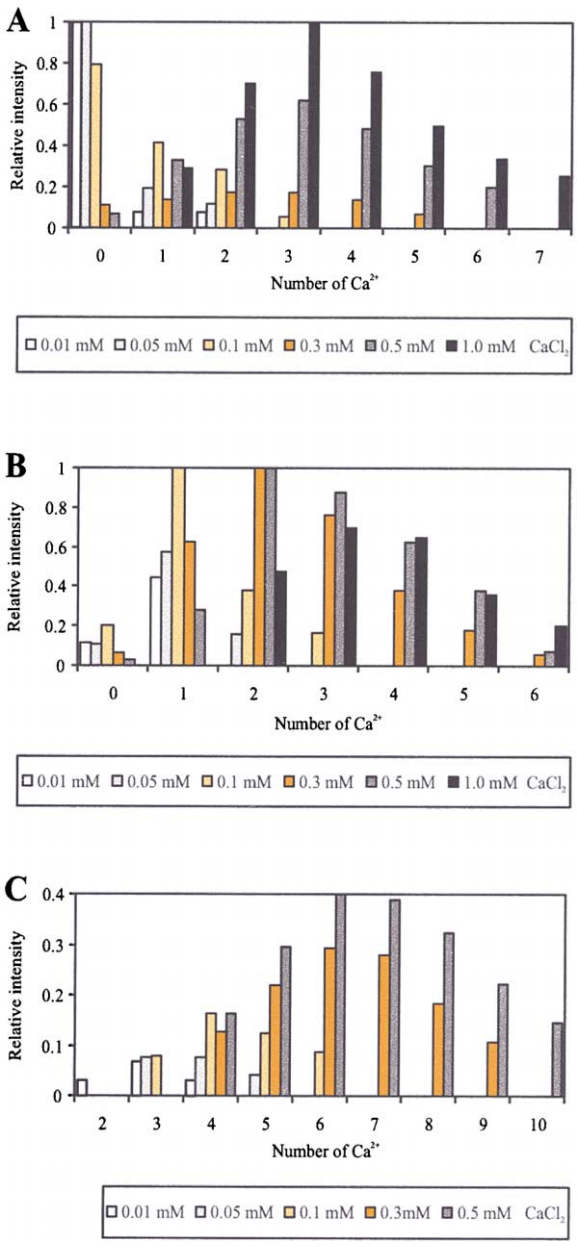

Figure 4. Calcium Binding to Monomeric and Dimeric OCN

Experimentally observed calcium binding patterns of monomeric OCN (A) in the absence and (B) in the presence of oxidation in the 4+ charge state in different $CaCl_2$ concentrations. The graphs show the relative intensity of each OCN–Ca_n and OCN-O-Ca_n species containing different numbers of associated Ca^{2+} ions. (C) Experimentally observed calcium binding patterns of dimeric OCN in the 7+ charge state in different $CaCl_2$ concentrations. The graph shows the relative intensity of each OCN_2-Ca_n species containing different numbers of associated Ca^{2+} ions. The concentration of OCN was kept at 15 μM in each experiment, and the solvent used was 5 mM ammonium acetate buffer at pH 5.8.

There was evidence of OCN binding at least seven Ca^{2+} ions. The major complex was OCN–Ca_3. OCN–O bound up to six Ca^{2+} ions, with the major complex being OCN–O–Ca_3.

Figure 4A represents Ca^{2+} binding to OCN for the 4+ charge state in ammonium acetate buffer at the different $CaCl_2$ concentrations. The maximum number of bound Ca^{2+} ions gradually increased up to seven as the $CaCl_2$ concentration increased. At the high $CaCl_2$ concentrations, the most abundant species was OCN–Ca_3. The closer study of Ca^{2+} binding illustrates that the abundances of the calcium bound species of OCN and OCN–O changed as a function of $CaCl_2$ concentration. The intensity of the Ca^{2+} binding pattern of OCN (see Figure 4A) decreased at the concentrations from 0.01 to 0.3 mM $CaCl_2$ and increased at 0.5 mM and 1.0 mM $CaCl_2$. In contrast, the abundance of Ca^{2+} bound species of OCN–O elevated from 0.01 to 0.5 mM concentrations but significantly diminished at 1.0 mM $CaCl_2$ (Figure 4B). The change between these two patterns of the calcium bound OCN species at different $CaCl_2$ concentrations could be explained by the hypothesis that Ca^{2+} binding to the protein occurs initially via an OCN–O form. The observed stoichiometry of the most abundant complex at 0.3 and 0.5 mM $CaCl_2$ (see Figures 4A and 4B) suggests that OCN has three high-affinity sites for Ca^{2+}. Since bovine OCN contains three Gla residues that are known to be required for Ca^{2+} to bind [8], it is reasonable to suppose that three Gla residues are occupied by Ca^{2+} in the OCN–Ca_3 complex. The results also indicate that after the three major Ca^{2+} binding sites are occupied, Ca^{2+} binding extends to the auxiliary metal binding sites and displaces the additional oxidation. This suggests that the oxidation was reversible and was removed during the occupation of the auxiliary metal binding sites.

A significant observation was the increased intensity of the noncovalent OCN dimer in the 7+ charge state as the $CaCl_2$ concentration was raised. The dimers contained either even or odd numbers of Ca^{2+}. Figure 4C shows the relative intensities for dimeric OCN in the 7+ charge state at different $CaCl_2$ concentrations. Dimers binding up to 10 Ca^{2+} ions were detected at 0.5 mM $CaCl_2$. Results at a concentration of 1.0 mM are not included in the graph because of lower signal quality that made interpretation of the spectra difficult. At 0.3 and 0.5 mM concentrations, the predominant species was a dimer associated with six Ca^{2+} ions. This indicates that the major monomeric species would be OCN having three Ca^{2+} binding sites occupied. The Ca^{2+} stoichiometry for the OCN dimer at each $CaCl_2$ concentration is therefore concluded to correlate well with the corresponding most abundant monomeric species (see Figures 4A and 4C). In addition, except for the result at 0.3 mM $CaCl_2$, there was a good correlation in the $CaCl_2$ concentration dependence of the dimer formation. On the basis of the spectra, the OCN monomer can be suggested to be in equilibrium with the OCN–O monomer as well as with the OCN dimer in solution.

Osteocalcins from a number of different species have been previously proposed to bind 2 mol of Ca^{2+} per mol of protein with relatively high affinity and, in addition, between 2 and 4 mol of Ca^{2+} with lower affinity. It has been shown [12] that the presence of Gla residues is necessary for high-affinity binding of Ca^{2+} to OCN and that decarboxylation of Gla residues suppresses Ca^{2+} binding to the protein and leads to the loss of protein activity. The space-filling model illustrated by Hauschka and Carr [12] suggests that Ca^{2+} coordination is pro-

vided through the carboxyl group of Gla. According to this model, Ca^{2+} binding to the first site is provided through Gla17, Gln39 and one tyrosine residue that has not been exactly assigned. The ligand residues for the coordination of the second Ca^{2+} ion are Gla24 and Glu31, and for the third Ca^{2+} ion they are Asp34, Gla17, Gla21, and Glu35, respectively. However, because the crystal structure of OCN is unsolved, the detailed assembly showing the geometry of the coordination around Ca^{2+} is not well defined. Our mass-spectrometric results indicate that OCN binds preferably 3 mol of Ca^{2+} per mol of OCN. The OCN–Ca_3 complex possibly represents OCN with all three Gla residues participating in Ca^{2+} coordination. Our postulation that Ca^{2+} ions would be bound through γ-carboxyl groups of Gla residues is supported by the observation that Ca^{2+} ions were lost at the same time as the loss of CO_2, i.e., decarboxylation of Gla, when the potential applied to the ESI capillary was increased. In other words, the metal ion, that is coordinated with relatively fragile γ-carboxyl structure, is lost during the fragmentation of this structure. We examined whether Ca^{2+} dissociates from calmodulin as readily as from OCN. The Ca^{2+} binding sites in calmodulin involve aspartic acid, glutamic acid, asparagine, and tyrosine in the Ca^{2+} binding loops of the EF-hand domains [35]. The experiments were done in the presence of RS20, a peptide derived from the phosphorylation site of smooth-muscle myosin light-chain kinase, which is shown to interact noncovalently with calmodulin. Sustained off-resonance irradiation (SORI) [36] and nozzle-skimmer experiments demonstrated that, in similar experimental conditions, the calmodulin-RS20-Ca_4 complex dissociated to the RS20 peptide and calmodulin-Ca_4, and that no dissociation of Ca^{2+} was observed. The reasoning for this is that Ca^{2+} binding in calmodulin takes place into unmodified amino acid residues, which are structurally more durable than Gla residues. On this account, the possibility that Ca^{2+} coordination has taken place in OCN without the participation of Gla can be dismissed. In addition, our observations establish clearly that the protein has several auxiliary sites for Ca^{2+} binding since there was evidence of the binding of as many as seven Ca^{2+} ions. Thus, the complex containing seven Ca^{2+} ions that formed at high $CaCl_2$ concentrations would correspond to complete occupation of the three Gla sites and four auxiliary sites.

At all $CaCl_2$ concentrations, the Ca^{2+} binding pattern of the protein conformed to a Gaussian distribution. An earlier CD and UV spectroscopic study carried out on bovine OCN has shown that the protein binds Ca^{2+} cooperatively [19]. The mass spectra of the Ca^{2+} binding pattern of bovine OCN indicate that in the experimental conditions used, there was no degree of significant cooperativity. ^1H NMR studies for bovine and rabbit OCN have suggested that the presence of Ca^{2+} does not induce a conformational transition, which would result a stable OCN structure. Instead, the Ca^{2+} bound structure in solution is flexible and labile; it has a diversity of locally fluctuating conformers with Ca^{2+} ions undergoing fast exchange [14, 20]. On the other hand, the additional Ca^{2+} equivalents in dog OCN are reported to stabilize the protein conformation induced by the association of first Ca^{2+} ions to the high-affinity sites of the protein

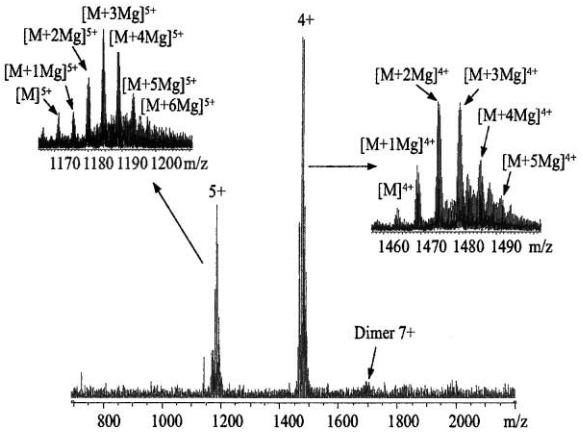

Figure 5. ESI-FTICR Mass Spectrum of OCN in the Presence of Magnesium

The data were recorded on a 15 μM protein and 0.5 mM $MgCl_2$ in 5 mM ammonium acetate buffer (pH 5.8). Insets show the expansion of the 5+ and 4+ charge states. M represents OCN.

[15]. Our observation that the abundance of the dimer increased with increasing $CaCl_2$ concentration implies that the additional Ca^{2+} ions give the monomer an enhanced capability for protein aggregation. The view of the structure obtained by spectroscopic methods gives an average structure that includes a diversity of multiple locally exchanging conformers with different numbers of Ca^{2+} ions occupied. Mass-spectrometric assignments made from the charge state distribution or the ligand binding pattern of the protein cannot alone produce a detailed insight into the local conformational movements if the charge state distribution remains the same in two or more conformations of the labile protein structure.

Mg^{2+} Binding to OCN

The ESI-FTICR mass spectrum of OCN after the addition of 0.5 mM $MgCl_2$ is shown in Figure 5 (the OCN/$MgCl_2$ concentration ratio was 1:33). The mass difference between the two consecutive Mg^{2+}-containing species was 21.973 u, showing that each Mg^{2+} ion displaced two protons from the protein (the theoretical mass difference was 21.969 u). As the concentration of $MgCl_2$ in the samples was high, the possibility of Na^+ being mistaken in Mg^{2+} was rejected. OCN analyzed in the presence of $MgCl_2$ gives rise to a series of peaks corresponding in mass to the protein associated with Mg^{2+} ions but without oxygen and residual Ca^{2+}. The results indicate that the binding of Mg^{2+} to OCN-O-Ca was significantly weaker than the binding of Ca^{2+}. At least six Mg^{2+} ions were observed to bind to the protein in the absence of oxidation and Ca^{2+} in both 5+ and 4+ charge states, and the shape of the ion binding pattern resembled Gaussian distribution, as was the case in the presence of Ca^{2+}. The major complex followed 1:3 protein-to-cation stoichiometry, as it did in the presence of Ca^{2+}.

Comparison of the overall charge state distribution of the OCN monomer in the presence or absence of Ca^{2+} and Mg^{2+} shows that neither of the cations had noticeable influence on the abundances of the charge states

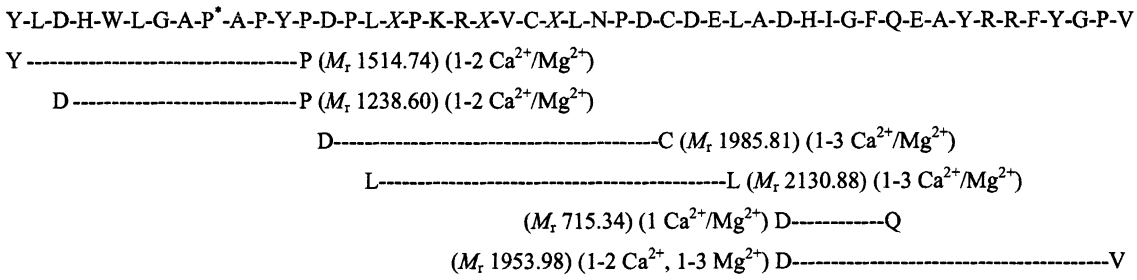

Figure 6. The Amino Acid Sequence of the Intact Bovine OCN and the Sequences of the Major OCN Peptides Identified by ESI-FTICR MS after Endoproteinase Asp-N Digestion

The first and last amino acid residues of each peptide are marked with a capital letter. P* represents hydroxyproline, and *X* represents γ-carboxyglutamic acid. The experimentally determined relative molecular masses and the numbers of associated Ca^{2+} and Mg^{2+} ions are given in parentheses. The amino acid sequence of OCN is as reported by Price et al. [43].

of the monomer. In contrast, the addition of Mg^{2+} did not influence dimer formation. A weak signal corresponding to the OCN dimer was detected in the presence of Mg^{2+}. However, closer analysis of the signal showed that none of the dimeric species in the pattern had been formed by purely Mg^{2+}-containing monomers because each dimer contained at least one Ca^{2+} ion and one monomer that was incorporated with oxygen. An earlier study has shown that Mg^{2+} induces an aberrant α-helical conformation in OCN [12] and therefore inhibits its binding to hydroxyapatite [18]. If it is assumed that the influence of Mg^{2+} on the divergent α-helicity of OCN can result in a form that has a decreased capacity for interaction with hydroxyapatite, the result indicates that Mg^{2+} also inhibits OCN dimerization, probably because of the formation of an unsuitable conformation of the protein [37].

Evidences for Differences in Ca^{2+} and Mg^{2+} Binding

Due to the binding strength difference of OCN for Mg^{2+} and Ca^{2+} in the absence and presence of oxygen atom and a residual Ca^{2+} ion, it could be assumed that Mg^{2+} may not bind to the same sites as Ca^{2+}. In order to investigate the differences in Ca^{2+} and Mg^{2+} binding, we dissociated the complexes in the gas phase by increasing the potential applied to the ES ion source capillary. The dissociation of metal ion took place concurrently with decarboxylation of Gla residues, which clearly showed that merely Gla–Ca^{2+} interaction has been responsible for most of the interaction between the protein and Ca^{2+} in the gas phase. The loss of three Ca^{2+} ions and three CO_2 molecules occurred at relatively low potential, which is comparable with the stability of γ-carboxylation of Gla residues. At the capillary potential of 128 V, the remaining metal complex detected was that due to (OCN-Mg)-3CO_2 in the case of the Mg^{2+}-containing sample and that due to (OCN-O-Ca)-3CO_2 in the case of the corresponding Ca^{2+}-containing sample. The results confirmed our hypothesis about the association of at least one Mg^{2+} ion of relatively high affinity for the auxiliary site that involves acidic side chains of residues other than Gla.

Ca^{2+} and Mg^{2+} Binding to Asp-N-Digested OCN Peptides

We used endoproteinase Asp-N to enzymatically digest OCN to further study metal binding to different parts of the protein. The digestion was done in the presence of Ca^{2+} or Mg^{2+}, and the peptides from the mixture were analyzed by ESI-FTICR MS. The digestion produced both specific and nonspecific reaction products, ranging in relative molecular mass from 700 to 3500. The peptides covered the whole sequence of the intact OCN. The posttranslational modifications characteristic of OCN were preserved. The peptides were unambiguously identified according to their monoisotopic masses. The major peptides and the numbers of Ca^{2+} and Mg^{2+} ions bound to them are presented in Figure 6. The N-terminal part of the sequence bound one to two Ca^{2+} or Mg^{2+} ions, whereas the middle part of the sequence bound up to three metal ions. The C-terminal part of the sequence bound up to two Ca^{2+} and one to three Mg^{2+} ions. There was no mass shift of 53.91 u in any of these peptides. The maximum number of Ca^{2+} ions bound to the peptides was in good agreement with the metal binding experiments performed with the intact protein, whereas the Mg^{2+} ions bound in slightly higher amounts to the peptides than to the intact protein. The tendency of the C-terminal sequence to bind higher numbers of Mg^{2+} ions may indicate that this part of the protein contains a Mg^{2+}-specific site. However, the fact that the intact protein in the folded three-dimensional form binds its ligands differently than the short peptides must be taken into account, and thus the results obtained with OCN and its peptides cannot be directly compared.

La^{3+} Binding to Bovine OCN

We used La^{3+} as a metal cation substrate for bovine OCN to determine whether the trivalent and physiologically nonspecific cation has an OCN binding affinity similar to those of Ca^{2+} and Mg^{2+}. Studies of Tb^{3+} and La^{3+} binding to chicken OCN [38] and Lu^{2+} binding to dog OCN [15] have shown that these ions are good calcium analogs for OCN studies. The association of 2 mol of La^{3+} per mol of protein has been demonstrated to occur tightly and to induce a calcium-like α-helical conformation in the protein. The concentration of $LaCl_3$ was increased up to 0.4 mM. At higher $LaCl_3$ concentrations

the salt produced clusters giving signals of high intensity and making the interpretation of the spectra difficult. La^{3+} must have bound to OCN by displacing three protons because the mass difference of the two consecutive La^{3+}-containing species was 135.878 u (the theoretical value being 135.883 u). At 0.4 mM $LaCl_3$, the binding of up to three La^{3+} ions was observed in OCN. The species OCN-O-Ca-La in the 4+ charge state gave the most intensive peak in the spectrum. OCN dimerization was not observed to occur in the presence of La^{3+}. Because the relative abundance of the La^{3+}-bound OCN and the number of La^{3+} bound to the protein were lower than in the case of the comparable Ca^{2+} or Mg^{2+} bound species, it was concluded that the affinity of the protein for La^{3+} was significantly lower than its affinity for Ca^{2+} or Mg^{2+}. Further studies, including the use of negative ion mode, may provide complementary information on the OCN-metal ion interactions and the differences in La^{3+}, Mg^{2+}, and Ca^{2+} binding.

Significance

This work provides the first mass spectrometric evidence of metal binding to the Gla-containing bone protein osteocalcin and, similarly, emphasizes the potential of ESI-FTICR mass spectrometry in aiding the investigation of the stoichiometry of protein-metal ion complexes. The association of different numbers of Ca^{2+}, Mg^{2+}, and La^{3+} ions into OCN and the formation of the OCN dimer from folded monomeric species were clearly distinguished. The number of Ca^{2+} ions associated with OCN was consistent with the number of the major Ca^{2+} binding sites in the protein. We showed that although the extent of Ca^{2+} and Mg^{2+} binding to OCN was uniform, only increasing the proportion of Ca^{2+} ions induced the dimerization of OCN. The observed phenomenon suggests an additional insight into the behavior of OCN and into a biological role of Ca^{2+} and Mg^{2+} ions in influencing the state of this bone protein. Moreover, the study underlines the power of FTICR mass spectrometry to identify in high resolution protein-ligand and multiprotein assemblies from small amounts of sample. Despite the different environments of the protein in gas and condensed phases, results obtained in the gas phase can give new binding information characteristic of the protein in condensed phases.

Experimental Procedures

Protein Isolation and Purification

Bovine OCN was isolated from bovine bone powder by solid phase extraction, gel filtration, and liquid chromatography on an anion-exchange column and purified by RP-HPLC on a Vydac C_{18} semi-preparative column as previously described [7, 39]. The purified protein was freeze-dried and stored at −20°C.

Sample Preparation for MS Analysis

OCN powder (0.5 mg) was dissolved in 1 ml of ultrapure water (Elga system) and further purified on a PD-10 column (Pharmacia Biotech, Uppsala, Sweden) that had been equilibrated in advance with ammonium acetate buffer (5 mM, pH 5.8). Metal stock solutions were prepared from $CaCl_2$, $MgCl_2$, and $LaCl_3$ (Sigma) by dissolving the salt in ultrapure water to a concentration of 40 mM. Appropriate aliquots of OCN and metal ion stock were mixed to reach the desired molar ratio. The final concentration of OCN was kept at 15 μM in electrospray samples. The samples were diluted with either water/acetonitrile (1/1, v/v) containing 1% formic acid or ammonium acetate buffer (5 mM, pH 5.8).

Preparation of Peptides from Osteocalcin by Asp-N Digestion

The purified protein (75 μg) dissolved in 150 μl of 10 mM ammonium acetate buffer (pH 6.8) and containing 1 mM $CaCl_2$ or $MgCl_2$ was incubated with 0.1% w/w of endoproteinase Asp-N (Sigma) by weight for 2 hr at 37°C. The reaction was stopped by the addition of 0.5 μl of formic acid, and the sample was diluted with water and buffer to obtain a protein concentration of 20 μM, a metal concentration of 0.25 mM, and an ammonium acetate concentration of 5 mM. The peptides were analyzed immediately after the enzymatic reaction.

Electrospray Ionization Fourier Transform Ion Cyclotron Resonance Mass Spectrometry

Mass spectrometry analyses of intact OCN were performed with a FTICR mass spectrometer (Bruker Daltonics, Billerica, MA, USA) equipped with a shielded 9.4 T superconducting magnet (Magnex Scientific Ltd., Abingdon, UK), a cylindrical infinity ICR cell (diameter d = 0.06 min), and an external ESI source (Analytica of Branford, Branford, CT, USA). This instrument has been described previously [40, 41]. In the ICR cell a typical background pressure was 2×10^{-10} mbar. The capillary and skimmer potentials were 64 V and 3 V, respectively, at which values the fully carboxylated OCN and its metal complexes were preserved in the gas phase. For ion source CID measurements, we gradually increased the potential of the capillary to obtain information on the fragmentation sensitivity of the protein. The flow rate of the sample solution into the electrospray ionization source was 0.83 μl min^{-1}. Carbon dioxide was used as a drying gas. Ions were accumulated for 4 s prior to extraction into the ICR cell. The ions were trapped in the cell, and all ions present were detected simultaneously by the use of appropriate excitation fields. Mass spectrometry analyses of Asp-N-digested samples were carried out with a FTICR mass spectrometer similar to the instrument described above except that it was equipped with a 4.7 T magnet and an off-axial spray needle. The flow rate of the sample solution was 4.17 μl min^{-1}, and nitrogen was used as a drying gas. The instrument has been described before [42]. We performed the experiments twice to ascertain repeatability and reliability of the results.

Acknowledgments

We thank Ms. Pia Keinänen for the isolation and purification of osteocalcin. We also thank Drs. Arja Pirhonen and Annikka Linnala-Kankkunen for help in different phases of this work. This work was supported by grants from the Protein Structure and Function Graduate School and the Graduate School of Bioorganic Chemistry (Ministry of Education, Finland), Academy of Finland (44213, 44906), and the Biotechnology and Biological Sciences Research Council (BBSRC) (88/9708907). The University of Warwick FTICR mass spectrometry facility is a United Kingdom National Facility supported by the Biotechnology and Biological Sciences Research Council and the Engineering and Physical Sciences Research Council (EPSRC).

Received: May 10, 2001
Revised: October 15, 2001
Accepted: October 30, 2001

References

1. Hauschka, P.V., Lian, J.B., Cole, D.E.C., and Gundberg, C.M. (1989). Osteocalcin and matrix Gla protein: vitamin K-dependent proteins in bone. Physiol. Rev. *69*, 990–1047.
2. Price, P.A., Williamson, M.K., Haba, T., Dell, R.B., and Jee, W.S.S. (1982). Excessive mineralization with growth plate closure in rats on chronic warfarin treatment. Proc. Natl. Acad. Sci. USA *79*, 7734–7738.
3. Brown, J.P., Delmas, P.D., Malaval, L., Edouard, C., Chapuy,

M.C., and Meunier, P.J. (1984). Serum bone Gla-protein: a specific marker for bone formation in postmenopausal osteoporosis. Lancet *1*, 1091–1093.

4. Ugar, D.A., and Karaca, I. (1999). Serum osteocalcin as a biochemical bone formation marker. Biochem. Arch. *15*, 379–382.
5. Roach, H.I. (1994). Why does bone matrix contain non-collagenous proteins? The possible roles of osteocalcin, osteonectin, osteopontin and bone sialoprotein in bone mineralisation and resorption. Cell Biol. Int. *18*, 617–628.
6. Ducy, P., Desbois, C., Boyce, B., Pinero, G., Story, B., Dunstan, C., Smith, E., Bonadio, J., Goldstein, S., Gundberg, C., et al. (1996). Increased bone formation in osteocalcin-deficient mice. Nature *382*, 448–452.
7. Kaartinen, M.T., Pirhonen, A., Linnala-Kankkunen, A., and Mäenpää, P.H. (1997). Transglutaminase-catalyzed cross-linking of osteopontin is inhibited by osteocalcin. J. Biol. Chem. *272*, 22736–22741.
8. Price, P.A., Williamson, M.K., and Lothringer, J.W. (1981). Origin of the vitamin K-dependent bone protein found in plasma and its clearance by kidney and bone. J. Biol. Chem. *256*, 12760–12766.
9. Houben, R.J.T.J., Jin, D., Stafford, D.W., Proost, P., Ebberink, R.H.M., Vermeer, C., and Soute, B.A.M. (1999). Osteocalcin binds tightly to the γ-glutamylcarboxylase at a site distinct from that of the other known vitamin K-dependent proteins. Biochem. J. *341*, 265–269.
10. Poser, J.W., Esch, F.S., Ling, N.C., and Price, P.A. (1980). Isolation and sequence of the vitamin K-dependent protein from human bone. Undercarboxylation of the first glutamic acid residue. J. Biol. Chem. *255*, 8685–8691.
11. Huq, N.L., Teh, L.C., Christie, D.L., and Chapman, G.E. (1984). The amino acid sequences of goat, pig and wallaby osteocalcins. Biochem. Int. *8*, 521–527.
12. Hauschka, P.V., and Carr, S.A. (1982). Calcium-dependent α-helical structure in osteocalcin. Biochemistry *21*, 2538–2547.
13. Hauschka, P.V., and Wians, F.H., Jr. (1989). Osteocalcin-hydroxyapatite interaction in the extracellular organic matrix of bone. Anat. Rec. *224*, 180–188.
14. Atkinson, R.A., Evans, J.S., Hauschka, P.V., Levine, B.A., Meats, R., Triffitt, J.T., Virdi, A.S., and Williams, R.J.P. (1995). Conformational studies of osteocalcin in solution. Eur. J. Biochem. *232*, 515–521.
15. Isbell, D.T., Du, S., Schroering, A.G., Colombo, G., and Shelling, J.G. (1993). Metal ion binding to dog osteocalcin studied by ^{1}H NMR spectroscopy. Biochemistry *32*, 11352–11362.
16. Delmas, P.D., Stenner, D.D., Romberg, R.W., Riggs, B.L., and Mann, K.G. (1984). Immunochemical studies of conformational alterations in bone γ-carboxyglutamic acid containing protein. Biochemistry *23*, 4720–4725.
17. Iwami, K., Dohi, Y., Moriyama, T., and Hamaguchi, K. (1987). Metal binding and metal-induced conformational change of frog bone γ-carboxyglutamic acid-containing protein. J. Biochem. *102*, 75–82.
18. Wians, F.H., Jr., Krech, K.E., and Hauschka, P.V. (1983). Effects of magnesium and calcium on osteocalcin adsorption to hydroxyapatite. Magnesium *2*, 83–92.
19. Gundlach, G., and Voegeli, R. (1983). Conformational changes of 4-carboxyglutamic acid-containing protein from bovine bone by binding of alkaline earth ions. Hoppe-Seyler's Z. Physiol. Chem. *364*, 31–39.
20. Prigodich, R.V., O'Connor, T., and Coleman, J.E. (1985). ^{1}H, ^{113}Cd, and ^{31}P NMR of osteocalcin (bovine γ-carboxyglutamic acid containing protein). Biochemistry *24*, 6291–6298.
21. Yamashita, M., and Fenn, J.B. (1984). Electrospray ion source. Another variation on the free-jet theme. J. Phys. Chem. *88*, 4451–4459.
22. Fenn, J.B., Mann, M., Meng, C.K., Wong, S.F., and Whitehouse, C.G. (1989). Electrospray ionization for mass spectrometry of large biomolecules. Science *246*, 64–71.
23. Pitt, A.R. (1998). Application of electrospray mass spectrometry in biology. Nat. Prod. Rep. *15*, 59–72.
24. Loo, J.A. (1997). Studying noncovalent protein complexes by electrospray ionization mass spectrometry. Mass Spectrom. Rev. *16*, 1–23.
25. Comisarow, M.B., and Marshall, A.G. (1974). Fourier transform ion cyclotron resonance spectroscopy. Chem. Phys. Lett. *25*, 282–283.
26. Marshall, A.G., Hendrickson, C.L., and Jackson, G.S. (1998). Fourier transform ion cyclotron resonance mass spectrometry: a primer. Mass Spectrom. Rev. *17*, 1–35.
27. Smith, R.D., Bruce, J.E., Wu, Q., and Lei, Q.P. (1997). New mass spectrometric methods for the study of noncovalent associations of biopolymers. Chem. Soc. Rev. *26*, 191–202.
28. Veenstra, T.D. (1999). Electrospray ionization mass spectrometry: a promising new technique in the study of protein/DNA noncovalent complexes. Biochem. Biophys. Res. Commun. *257*, 1–5.
29. Gaskell, S.J. (1997). Electrospray: principles and practice. J. Mass Spectrom. *32*, 677–688.
30. Nemirovskiy, O., Giblin, D.E., and Gross, M.L. (1999). Electrospray ionization mass spectrometry and hydrogen/deuterium exchange for probing the interaction of calmodulin and calcium. J. Am. Soc. Mass Spectrom. *10*, 711–718.
31. Veenstra, T.D., Johnson, K.L., Tomlinson, A.J., Kumar, R., and Naylor, S. (1998). Correlation of fluorescence and circular dichroism spectroscopy with electrospray ionization mass spectrometry in the determination of tertiary conformational changes in calcium-binding proteins. Rapid Commun. Mass Spectrom. *12*, 613–619.
32. Troxler, H., Kuster, T., Rhyner, J.A., Gehring, P., and Heizmann, C.W. (1999). Electrospray ionization mass spectrometry: analysis of the Ca^{2+}-binding properties of human recombinant α-parvalbumin and nine mutant proteins. Anal. Biochem. *268*, 64–71.
33. Nakamura, T., Yu, Z., Fainzilber, M., and Burlingame, A.L. (1996). Mass spectrometric-based revision of the structure of a cysteine-rich peptide toxin with γ-carboxyglutamic acid, TxVIIA, from the sea snail, *Conus textile*. Protein Sci. *5*, 524–530.
34. Kelleher, N.L., Zubarev, R.A., Bush, K., Furie, B., Furie, B.C., McLafferty, F.W., and Walsh, C.T. (1999). Localization of labile posttranslational modifications by electron capture dissociation: the case of γ-carboxyglutamic acid. Anal. Chem. *71*, 4250–4253.
35. Babu, Y.S., Bugg, C.E., and Cook, W.J. (1988). Structure of calmodulin refined at 2.2 Å resolution. J. Mol. Biol. *204*, 191–204.
36. Nousiainen, M., Vainiotalo, P., Feng, X., and Derrick, P.J. (2001). Calmodulin-RS20-Ca_4 complex in the gas phase: electrospray ionisation and Fourier transform ion cyclotron resonance. Eur. J. Mass Spectrom. *7*, 393–398.
37. Lafitte, D., Heck, A.J.R., Hill, T.J., Jumel, K., Harding, S.E., and Derrick, P.J. (1999). Evidence of noncovalent dimerization of calmodulin. Eur. J. Biochem. *261*, 337–344.
38. Hauschka, P.V., and Gallop, P.M. (1977). Purification and calcium-binding properties of osteocalcin, the γ-carboxyglutamate-containing protein of bone. In Calcium-Binding Proteins and Calcium Function, R.H. Wasserman, R.A. Corradino, E. Carafoli, R.H. Kretsinger, D.H. MacLennan, and F.L. Siegel, eds. (New York: Elsevier North-Holland), pp. 338–347.
39. Colombo, G., Fanti, P., Yao, C., and Malluche, H.H. (1993). Isolation and complete amino acid sequence of osteocalcin from canine bone. J. Bone Miner. Res. *8*, 733–743.
40. Hill, T.J., Lafitte, D., Wallace, J.I., Cooper, H.J., Tsvetkov, P.O., and Derrick, P.J. (2000). Calmodulin-peptide interactions: apocalmodulin binding to the myosin light chain kinase target-site. Biochemistry *39*, 7284–7290.
41. Palmblad, M., Håkansson, K., Håkansson, P., Feng, X., Cooper, H.J., Giannakopulos, A.E., Green, P.S., and Derrick, P.J. (2000). A 9.4T Fourier transform ion cyclotron resonance mass spectrometer: description and performance. Eur. J. Mass Spectrom. *6*, 267–275.
42. Nuutinen, J.M.J., Irico, A., Vincenti, M., Dalcanale, E., Pakarinen, J.M.H., and Vainiotalo, P. (2000). Gas-phase ion-molecule reactions between a series of protonated diastereomeric cavitands and neutral amines studied by ESI-FTICRMS: gas-phase inclusion complex formation. J. Am. Chem. Soc. *122*, 10090–10100.
43. Price, P.A., Poser, J.W., and Raman, N. (1976). Primary structure of the γ-carboxyglutamic acid-containing protein from bovine bone. Proc. Natl. Acad. Sci. USA *73*, 3374–3375.